Improving InGaN-LED performance by optimizing the patterned sapphire substrate shape*

Huang Xiao-Hui(黄小辉), Liu Jian-Ping(刘建平), Fan Ya-Ming(范亚明), Kong Jun-Jie(孔俊杰), Yang Hui(杨 辉), and Wang Huai-Bing(王怀兵)†

Suzhou Institute of Nano-Tech and Nano-Bionics, Chinese Academy of Sciences, Suzhou 215125*, China*

(Received 26 November 2011; revised manuscript received 15 March 2011)

The epitaxial growths of GaN films and GaN-based LEDs on various patterned sapphire substrates (PSSes) with different values of fill factor (f) and slanted angle (θ) are investigated in detail. The threading dislocation (TD) density is lower in the film grown on the PSS with a smaller fill factor, resulting in a higher internal quantum efficiency (IQE). Also the ability of the LED to withstand the electrostatic discharge (ESD) increases as the fill factor decreases. The illumination output power of the LED is affected by both θ and f. It is found that the illumination output power of the LED grown on the PSS with a lower production of $\tan\theta$ and f is higher than that with a higher production of $\tan\theta$ and f.

Keywords: GaN, Patterned sapphire substrate, light emitting diode

PACS: 71.55.Eq, 78.30.Fs **DOI:** 10.1088/1674-1056/21/3/037105

1. Introduction

Group III-nitride-based semiconductors have been recently used as high-brightness light emitting diodes (LEDs) and lasers in large-area full-color outdoor displays, signal light, and high performance back lighting units in liquid crystal displays with emission in the near-ultraviolet, blue, and green spectral regions.[1,2] Though high brightness GaN-based LEDs are commercially available, threading dislocations (TDs) with a density of 10^8–$10^9/\mathrm{cm}^2$ remain in the LED structures due to the large differences of lattice constant and thermal expansion coefficient between the GaN epi-layer and the sapphire substrate. The external quantum efficiency (EQE) of the InGaN LED is still not large enough compared with the expected value. The EQE is the production of injection efficiency, internal quantum efficiency (IQE), and light extraction efficiency (LEE). It is related to the substrate property and the epi-layer quality. It is also related to the substrate shape, the chip processing, the die geometry, and the package construction. Improving both IQE and LEE has thus become the focus of researches. Many techniques have been developed to improve the quality of the epi-layers, such as epitaxial lateral overgrowth (ELOG),[3] surface roughening,[4,5] nanoimprinting,[6] SiN nanonetwork,[7] and porous TiN.[8] Although those techniques can effectively improve the crystalline quality, the two-step regrowth procedures involved make them rather time-consuming and easy to introduce contaminations in the epilayers.

Currently, GaNbased LEDs grown on patterned sapphire substrates (PSSes) have been studied by more and more researchers.[9,10] The PSS, which is a mask-free and therefore contamination-free method, reduces the threading dislocation density in the GaN epilayers and enhances the light extraction efficiency of the LED. The TD density reduces significantly due to the introduction of the ELOG and its combination with the selective area growth (SAG) in the epitaxial processes on the PSS.[11] And the use of the PSS enhances the light extraction efficiency due to the increased light scattering.[12] Many types of PSSes have been studied and successfully applied to the fabrications of high-efficiency LEDs.[13,14] And there are a lot of reports focusing on the comparisons of the EQE between the LEDs based on the un-patterned sapphire substrate (un-PSS) and the PSS.[15,16]

In this work, periodic pyramidal array PSSes with varying fill factors and slanted angles are used as GaN-based LED substrates. The epi-layers quality, the

*Project supported by the National Natural Science Foundation of China (Grant Nos. 61006084 and 61076119) and the Technical Corporation Innovation Foundation of Suzhou Industrial Park, China (Grant No. SG0962).

†Corresponding author. E-mail: hbwang2006@sinano.ac.cn

© 2012 Chinese Physical Society and IOP Publishing Ltd

microstructure, and the optical properties of the InGaN/GaN LED are systematically investigated.

2. Experiment

The PSSes were prepared by inductively coupled plasma (ICP) etching. The surface morphologies of the PSS surfaces were characterized by scanning electron microscopy (SEM) as shown in Fig. 1. Four types of PSSes were prepared with their diameter/spacing/height being 2.0 μm/1.0 μm/1.5 μm, 3.0 μm/2.0 μm/1.5 μm, 3.0 μm/1.0 μm/1.8 μm, and 3.75 μm/1.25 μm/1.8 μm, and were called PSS-I, PSS-II, PSS-III, and PSS-IV, respectively. The slanted angles (θ_s) of these sidewalls were calculated from $\tan\theta_s = 2$ height/diameter to be 56.3°, 45°, 50.2°, and 43.8° for the four kinds of substrates, respectively.

The LED structure grown by using the metal-organic chemical vapour deposition was comprised of a 25 nm nucleation layer on the PSS, a 1.5 μm undoped-GaN layer film, a 2.0 μm n-GaN layer, a five-period InGaN/GaN multiple quantum well (MQW) with the emission wavelength in the blue region (460 nm), a 20 nm Mg-doped AlGaN electron blocking layer, and a 150 nm p-GaN layer. Trimethylgallium (TMGa) and ammonia gas (NH_3) were used as precursors for Ga and N sources, respectively. Hydrogen (H_2) was used as the carrier gas in each growth run except that nitrogen (N_2) was used as the carrier gas for growing the MQW layers.

The device mesa with a chip size of 350 μm× 350 μm was then determined by the inductively coupled plasma to remove the Mg-doped GaN layer and the MQW until the Si-doped GaN layer was exposed. The indium tin oxide (ITO) layer was deposited to form a p-side contact layer and a current spreading layer. The Cr/Au layer was deposited on the ITO layer to form the p-side and the n-side electrodes.

The surface morphologies and the structural properties of the GaN films were characterized by cathodoluminescence (CL), scanning electron microscopy (SEM), transmission electron microscopy (TEM), and X-ray diffraction (XRD). The optical and the electrical properties of the LEDs were tested by electroluminescence (EL), electrostatic discharge (ESD), and output power–current (L–I) characteristics.

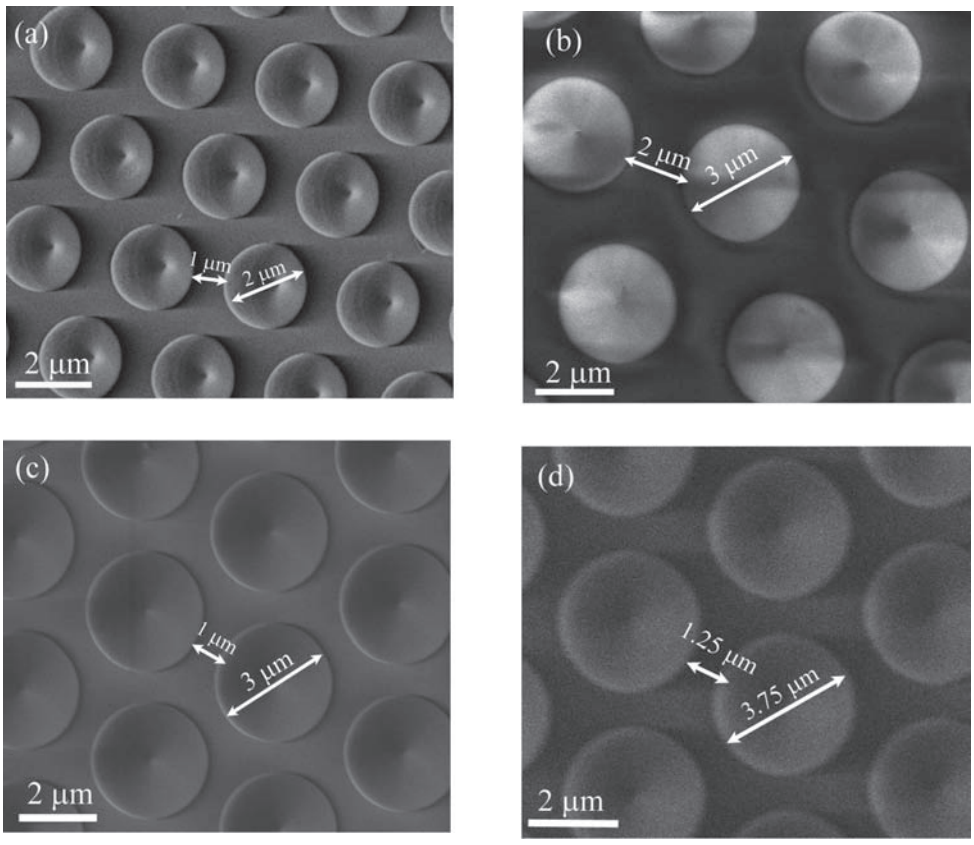


Fig. 1. Plan-view SEM images of (a) PSS-I, (b) PSS-II, (c) PSS-III, and (d) PSS-IV.

3. Results and discussion

There are planar and slanted areas in these PSSes as shown in Fig. 1. The fraction of the planar growth area can be estimated by the fill factor (F), which represents the area ratio of the GaN growth on the PSS

$$F = \text{planar area/total area}. \quad (1)$$

The F values for PSS-I, PSS-II, PSS-III, and PSS-IV are 59.7%, 67.4%, 49%, and 49%, respectively. The essential role of the low temperature (LT) GaN as a nucleation layer is to supply a high density of nucleation centers with the same orientation and to promote the lateral growth of the epitaxial film by decreasing the interfacial free energy between the epitaxial film and the substrate.[17] Figure 2 shows the SEM images of the epilayers grown on PSS-II with the LT-GaN nucleation layer at 530 °C for various growth times: (a) 0 min, (b) 3 min, (c) 10 min, and (d) 30 min. The growth selectively proceeds with the GaN islands nucleating at specific locations rendered by the pattern. In the initial growth stage of GaN on PSS-II, the GaN nucleation islands (NIs) grow predominantly on the flat trench around the cones despite the LT-buffer layer deposited on the surfaces of the cones. The large GaN NIs formed around the cones cover the small GaN NIs formed in the trench area in Fig. 2(b) The NIs start to coalesce at the trench as the growth continues, as shown in Fig. 2(c). It can be observed that the GaN on the PSS shows a hexagonal growth when the growth time increases to 30 min as shown in Fig. 2(d). Then the GaN gradually overgrows the protruding cones and coalesces near the summit as the growth time increases.[18]

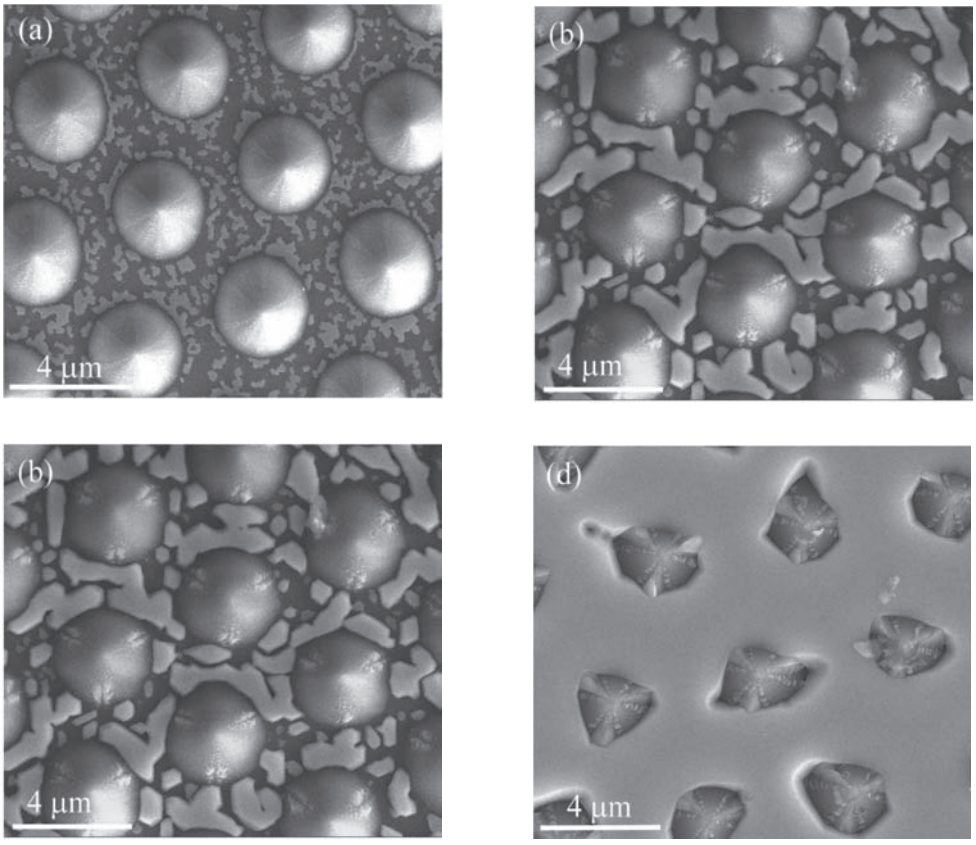


Fig. 2. Plan-view SEM images of GaN epi-layers grown on PSS-II. Growth times are 0 min, 3 min, 10 min, and 30 min for panels (a)–(d), respectively.

To investigate the crystal quality of the GaN films grown on these substrates, CL and TEM are employed to observe the dislocation distributions in the four GaN epi-layers each with a thickness of 3 μm. Figures 3(a)–3(d) show the plan-view CL intensity spatial mappings of the GaN films on PSS-I, PSS-II, PSS-III, and PSS-IV, respectively. The dark region in the band-edge luminescence mapping of the GaN film can be attributed to the non-radiative recombination at the threading dislocations caused by the deficiency

of minority carriers.[19] The densities of the dark regions are estimated to be 4×10^8 cm^{-2}, 5×10^8 cm^{-2}, 1.2×10^8 cm^{-2}, and 1×10^8 cm^{-2}, respectively, which are consistent with the tendency of fill factor F of these PSSes. The bright regions, which represent the areas of low dislocation density, appear at the places corresponding to the un-planar areas of the PSS. It is also testified by the cross-sectional TEM of the epi-layer grown on PSS-II (Fig. 3(e)), which is obtained for $g = [0002]$. The TDs propagate mainly in the planar regions, and there exist a few TDs on the sidewall and the top surface of the cone, which indicates that the larger the fill factor, the higher the TD density.

In addition to CL and TEM, XRD is used to evaluate the epi-layer crystal quality. The results are summarized in Table 1. The full widths at half-maximum of the rocking curves for both the symmetric (002) and the asymmetric (102) reflections decrease monotonically as the fill factor decreases from 67.4% to 49%. The difference between PSS-III and PSS-IV, each with a fill factor of 49%, is ascribed to the difference of the slanted angle. The structural quality of the epi-layer increases as the slanted angle decreases.[20] The improvement on the structural quality is also verified by the CL pattern density. The selected-area electron diffraction (SAED) pattern is taken from GaN on PSS-II (Fig. 3(f)), which shows that the GaN film has a wurtzite structure on c-sapphire.

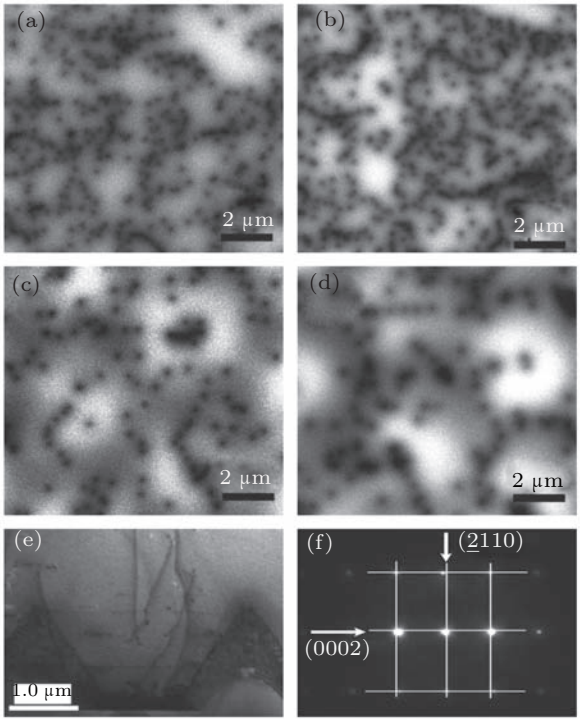


Fig. 3. Plan-view CL mappings of 3 μm epi-layers grown on (a) PSS-I, (b) PSS-II, (c) PSS-III, and (d) PSS–IV, (e) cross-sectional TEM of epi-layer grown on PSS-II with $g = [0002]$, and (f) selected-area electron diffraction pattern of GaN epi-layer grown on PSS-II.

Table 1. Parameters of epi-layer on PSS and performance of LED on PSS.

Type	Patterned sapphire substrates				Epi-layers on PSS			LED	
	Shape /μm×μm×μm	θ_s/°	F/%	χ	(002) /arcsec	(102) /arcsec	CL pattern density /10^8 cm^{-2}	ESD yield (2000 V) /%	LOP (20 mA) /mW
PSS-I	$2\times1\times1.5$	56.3	59.7	1.12	280	252	4	88.9	19.73
PSS-II	$3\times2\times1.5$	45	67.4	1.48	303	288	5	79.1	20.63
PSS-III	$3\times1\times1.8$	50.2	49	1.70	275	246	1.2	92.9	2170
PSS-IV	$3.75\times1.25\times1$	43.8	49	2.13	246	219	1	93.9	

The ability to withstand electrostatic discharge (ESD) is important for a GaN-based LED. In order to maintain or enhance the ESD characteristics, the pit-related TDs that inherently occur during the growth of the InGaN/GaN MQW and eventually terminate in the top surface of the LED should be minimized. Also it is widely believed that the TDs in GaN provide nonradiative recombination channels and charge leakage pathways.[21] So it is believed that the ESD can be improved by reducing the TD density. After the human body model (HBM) ESD 2000 V impulses have been applied to the LED chip on wafer (COW), the reverse current is measured under a reverse voltage of 5 V using a parameter analyzer. If the reverse current is over 1 μA, the chip is considered to be damaged by the ESD impulse. The data are obtained with a sampling rate of 50:1. The ESD yields of the GaN-based LEDs on the four PSSes are plotted in Fig. 4 with the CL dark density of the GaN epi-layers. There are more TDs found, and the CL dark density is higher with a larger fill factor, which worses the ESD yield, because there are larger and more leakage pathways

as the fill factor increases from 49% to 67.4%.

The use of PSS for LED growth is believed to be very promising, as it improves the IQE by reducing the TD density and enhances the LEE by increasing the light scattering.[22] The result from the Monte Carlo ray-tracing method shows that the LEE decreases down to approximate 50° with the increasing slanted angle.[23] It is a very important parameter of the PSS shape, which affects the EQE considerably. Based on our results, it is suggested that the EQE increases slightly as the slanted angle decreases down to about 44°. The study carried out by Cheng *et al.*[20] shows that both the crystal quality and the performance of the GaN-based LED increase by reducing the slanted angle of the PSS. However, the output power in our study does not increase linearly by reducing the slanted angle. It is believed that the output power of the LED is determined by both the fill factor and the slanted angle of the PSS.

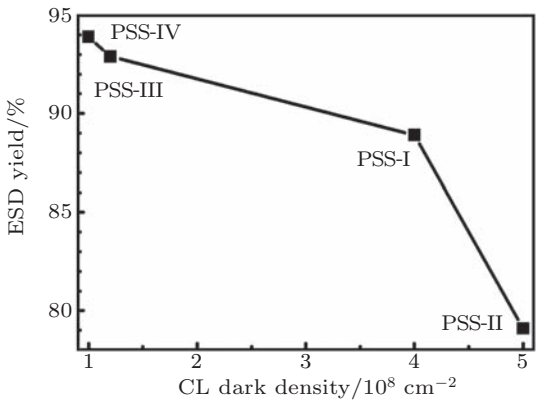


Fig. 4. ESD yield of LED chip as a function of CL dark density for GaN epi-layers grown on PSS-I, PSS -II, PSS –III, and PSS–IV. ESD data are obtained with sampling rate of 50:1.

In order to study the effect of the PSS shape on the output power systematically, we define a variable χ depending on both the slanted angle and the fill factor

$$\chi = 1/(\tan\theta_{\rm s} \times F). \tag{2}$$

The χ values are found to be 1.12, 1.48, 1.70, and 2.13 for these PSSes, as shown in Table 1. The output powers of the GaN-based LEDs grown on these PSSs are tested by a chip analyzer. The results are obtained as the average values with a same sampling rate of 50:1. Figure 5 shows the comparative observation between the χ value and the output power at a forward current of 20 mA. The output power of LED increases monotonically as the value of χ increases. The output power of the LED grown on PSS-IV with $\chi = 2.13$ is 20% higher than that grown on PSS-I with $\chi = 1.12$.

The plot shows that the output power of LED is not determined only by the slanted angle but also by the fill factor, which is coincident with the principle that the EQE is equal to the IQE multiplied by the LEE. Although the TDs are affected by the slanted angle to some extant due to the epitaxial regrowth occurring on the cone of the PSS, the TEM data above show that the TDs propagate primarily from the flat regions, and there are nearly no dislocations around the slanted surface. The dislocations act as the non-radiative centers which deteriorate the IQE. And the LEE is also related to the chip processing, the die geometry, and the package construction. We fabricate the bare chips with the same size in each chip processing run, so the LEE in our work is determined mainly by the PSS shape, i.e,. the slanted angle. It is concluded that the output power is determined by the combination of the slanted angle and the fill factor. The output power is higher with a smaller fill factor and a smaller slanted angle until 44°.

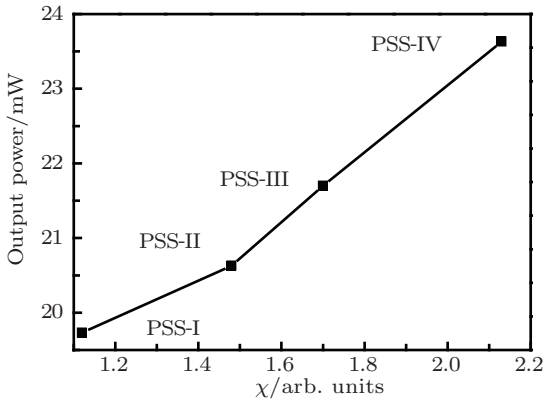


Fig. 5. Output power of LED versus χ at an injection current of 20 mA. Results are obtained as average values with same sampling rate of 50:1.

4. Conclusion

GaN film and GaN-based LED are grown on various PSSes with different fill factors and different slanted angles. The PSS shape affects the crystal quality of the GaN film and the performance of the GaN-based LED considerably. The TDs are lowered as the fill factor decreases, so the IQE is higher. The ESD yield of the LED chip is improved by reducing the fill factor. And the LEE is improved by reducing the slanted angle of the PSS. It is believed that the output powers of the LEDs on these PSSes are determined by both the fill factor and the slanted angle. The output

power of the LED on PSS-IV with a $\tan\theta_s \times F$ value of 2.13 is 20% higher than that grown on the PSS-I (1.12).

References

[1] Nakamura S, Senoh N, Iwasa N and Nagahama S I 1995 *Jpn. J. Appl. Phys.* **34** L797

[2] Zhang L Q, Zhang S M, Jiang D S, Wang H, Zhu J J, Zhao D G, Liu Z S and Yang H 2009 *Chin. Phys.* B **18** 5350

[3] Linthicum K, Gehrke T, Thomson D, Carlson E, Rajagopal P, Smith T, Batchelor D and Davis R 1999 *Appl. Phys. Lett.* **75** 196

[4] Peng W C and Wu Y S 2006 *Appl. Phys. Lett.* **88** 18117

[5] He A H, Zhang Y, Zhu X H, Chen X W, Fan G H and He M 2010 *Chin. Phys.* B **19** 068101

[6] Huang H, Lin C H, Yu C C, Chiu C H, Lai C F, Kuo H C, Leung K M, Lu T C, Wang S C and Lee B D 2008 *Nanotechnology* **19** 185301

[7] Wang T, Morishima Y, Naoi N and Sakai S 2000 *J. Cryst. Growth* **213** 188

[8] Moon X T, Xie J, Liu C, Fu Y, Ni X, Biyikli N, Zhu K, Yun F, Morkoc H, Sagar A and Feenstra R M 2006 *J. Cryst. Growth* **291** 301

[9] Tang T Y, Shiao Y, Lin C H, Shen K C, Huang J J, Ting S Y, Liu T C, Yang C C, Yao C L, Yeh J H, Hsu T C, Chen W C, Hsu H C and Chen L C 2009 *J. Appl. Phys.* **105** 023501

[10] Lee K T, Lee Y C and Chang J Y 2008 *J. Electrochem. Soc.* **155** H638

[11] Okada N, Murata T, Tadatomo K, Chang H C and Watanabe K 2009 *Jpn. J. Appl. Phys.* **48** 122103

[12] Gao H Y, Yan F W, Zhang Y, Li J M, Zeng Y P and Wang G H 2008 *Solid State Electron.* **52** 962

[13] Lin H C, Liu H H, Lee G Y, Chyi J I, Lu C M, Chao C W, Wang T C, Chang C J and Chi S W S 2010 *J. Electrochem. Soc.* **157** H304

[14] Lin H C, Lin R S, Chyi J I and Lee C M 2008 *IEEE Photon. Technol. Lett.* **20** 1621

[15] Song J C, Lee S H, Lee I H, Seol K W, Kannappan S and Lee C R 2007 *J. Cryst. Growth* **308** 321

[16] Lin H, Liu S, Zhang X S, Liu B L and Ren X C 2009 *Acta Phys. Sin.* **58** 959 (in Chinese)

[17] Akasaki I 2000 *J. Cryst. Growth* **221** 231

[18] Kim Y H, Ruh H, Noh Y K, Kim M D and Oh J E 2010 *J. Appl. Phys.* **107** 063501

[19] Rosner S J, Carr E C, Ludowise M J, Girolami G and Erikson H I 1997 *Appl. Phys. Lett.* **70** 420

[20] Cheng J H, Wu Y S, Liao W C and Lin B W 2010 *Appl. Phys. Lett.* **96** 051109

[21] McCarthy L, Smorchkova I, Xing H, Fini P, Keller S, Speck J, DenBaars S P, Rodwell M J W and Mishra U K 2001 *Appl. Phys. Lett.* **78** 2235

[22] Yamada M, Mitani T, Narukawa Y, Shioji S, Niki I, Sonobe S, Deguchi K, Sano M and Mukai T 2002 *Jpn. J. Appl. Phys.* **41** L1431

[23] Kim J B, Kim S M, Kim Y W, Kang S K, Jeon S R, Hwang N, Choi Y J and Chung C S 2010 *Jpn. J. Appl. Phys.* **49** 042102